Journal of Power Sources, 8 (1982) 229 - 255

REVIEW OF THE STRUCTURE AND THE ELECTROCHEMISTRY OF NICKEL HYDROXIDES AND OXY-HYDROXIDES

P. OLIVA, J. LEONARDI and J. F. LAURENT

S.A.F.T., 111, Bld Alfred Daney, 33000 Bordeaux (France)

C. DELMAS and J. J. BRACONNIER

Laboratoire de Chimie du Solide du CNRS, Université de Bordeaux I, 351, cours de la Libération, 33405, Talence Cédex (France)

M. FIGLARZ and F. FIEVET

Université Paris VII, Place Jussieu, 75251, Paris Cédex 05 (France)

A. de GUIBERT

C.G.E. (Laboratoire de Marcoussis), Route de Nozay, 91460, Marcoussis (France)

Summary

Particular emphasis is placed on the structural (and textural) characterization of the phases involved in nickel hydroxide electrodes as a prerequisite to a rational approach to their redox behaviour.

Recent chemical and electrochemical papers are discussed with the object of throwing some light on traditionally unexplored features of such electrodes.

Introduction

The remarkable cycling durability of nickel hydroxide electrodes (NOE) in alkaline cells has long been interpreted on the basis that a highly reversible redox transfer occurs between well defined active species. This is the reason why so much effort has been devoted to attempts to characterize the phases present within the electrode during charge and discharge.

In fact, progress in the understanding of solid-phase properties and transport mechanisms has now convinced experimentalists that continuous slight changes occur on cycling both in the electrochemical mechanisms and in the structures of the involved species, and that perfect control over NOE redox processes would still require years of investigation.

0378-7753/82/0000-0000/$02.75

Hence the general reaction scheme initially proposed by Bode *et al.*[1] *.

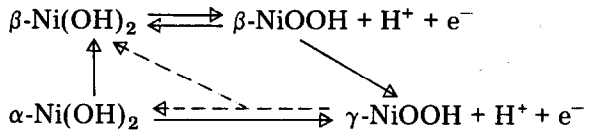

the validity of which is still unquestioned, must be acknowledged with sufficient flexibility in order not to ignore the prevailing influence of such parameters as electrolyte concentration and nature, material texture, charge and discharge rates, etc. . . ., on the electrochemical system.

The purpose of this paper is thus to propose a synthetic view of the subject through a close examination of all recent papers published both in the chemical and the electrochemical literature, and to complement previous reviews [2 - 6] by placing maximum emphasis on a structural interpretation of the NOE behaviour.

The following subjects will be dealt with:

A — Physico-chemical and structural characteristics of Ni(II) hydroxides.

B — Hydroxides and oxy-hydroxides with a nickel oxidation state higher than II.

C — Structural approach to the NOE behaviour.

D — Thermodynamic and kinetic approach to the NOE behaviour.

E — Role of the electrolyte.

F — Role of foreign cations.

A. Physico-chemical and structural characteristics of Ni(II) hydroxides

Early crystallographic studies established a marked distinction between "well crystallized" β-$Ni(OH)_2$, isomorphous with brucite, $Mg(OH)_2$, and compounds which can still be considered as Ni(II) hydroxides but which contain a variable excess of intersheet water (+ foreign ions) and exhibit low crystallinity.

The conventional α-$Ni(OH)_2$ denomination used for such compounds must then be taken as a general denomination for a large set of disordered Ni(II) hydroxides and does not represent a well defined polymorph of $Ni(OH)_2$. However, the similarity of trends observed in the electrochemical behaviour of all such disordered "α" hydroxides has induced electrochemists to adopt the same α–β dichotomy as crystallographers, and we shall thus adhere to such a convention in the present paper.

The different methods of preparation of nickel hydroxide have been reviewed by Oswald and Asper [7]. Nickel hydroxide does not tend to form large, well shaped crystals, and during its precipitation from aqueous salt solutions, well crystallized $Ni(OH)_2$ is not the primary product. Depending on experimental conditions either hydroxy-salts (basic salts) or poorly crystallized α-type hydroxides can be isolated as primary precipitation products. β-$Ni(OH)_2$ may then be obtained by ageing of such compounds [8 - 11], but always contain adsorbed foreign ions and water.

*— — — Dashed lines indicate partial reactions.

1. β-Ni(OH)$_2$

To obtain pure nickel hydroxide, NH_3 proves to be a much better precipitating reactant than strong alkali. Merlin's method [12] consists of adding an excess of ammonia to a nickel salt solution; on boiling, β-Ni(OH)$_2$ precipitates slowly from the Ni(II) hexaammine solution thus obtained. A particularly pure nickel hydroxide has also been prepared by Fievet and Figlarz [13, 14] *via* a two-step reaction: (i) precipitation of an α-type turbostratic hydroxide from ammonia and a nickel solution, (ii) hydrothermal treatment of this turbostratic hydroxide.

β-Hydroxide obtained by the latter method consists of hexagonal, platelike, submicronic particles (Fig. 1(a)). Selected area electron diffraction indicates that such hexagonal platelets are monocrystals lying on the (001) plane (Fig. 1(b)).

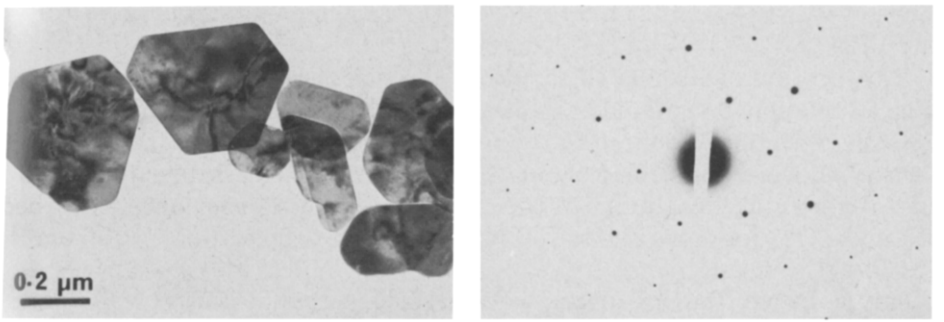

(a) (b)

Fig. 1. β-Ni(OH)$_2$ particles obtained by hydrothermal growth of an aqueous suspension of a turbostratic nickel hydroxide. (a) Electron microscopy; (b) selected area electron diffraction by one particle of sample (a).

Crystal structure

β-Ni(OH)$_2$ crystallizes in the hexagonal system ($P\bar{3}m1$–$D^3 3d$) common to several halogenides (CdI_2 type) and to other hydroxides M(OH)$_2$ (M = Ca, Mg, Fe, Co, Mn, Cd). The unit cell parameters are a = 3.126 Å and c = 4.605 Å [ASTM, 14 - 117].

The structure can be described as an hexagonal close-packed structure of hydroxyl ions (AB oxygen packing) with Ni(II) occupying octahedral interstices one plane out of two. It can also be visualized as a layered structure, each layer consisting of an hexagonal planar arrangement of Ni(II) ions with an octahedral coordination of oxygen, three oxygen atoms lying above the nickel plane, three lying below. The layers are stacked up along the c axis. By analogy with the structure of Mg(OH)$_2$ and Ca(OH)$_2$ the O—H bond is thought to be parallel to the c axis [18].

As evidenced by IR there is no hydrogen bonding between the OH groups of two adjacent layers [19].

Infrared and Raman spectra

A complete factor group analysis of crystals containing linear groups has been done by Mitra [20]. Each OH^- ion in the brucite-type structure occupies a C_{3v} site. Its internal and external normal vibrations form the basis of the representation $\Gamma = 2A_1 + 2E$.

All the centrosymmetric *g* modes are Raman active, whereas the antisymmetric *u* modes are excited in the infrared. Thus four bands can be seen both in the IR (Fig. 2) and the Raman spectra of β-$Ni(OH)_2$.

$Ni(OH)_2$ IR absorption has been thoroughly studied by Cabannes-Ott [21] in relation to the spectra of isomorphous $M(OH)_2$ hydroxides. The narrow band located near 3650 cm^{-1} is characteristic of the stretching vibration ν_{OH} of non-hydrogen-bonded OH groups. The three other bands are located in the 700 - 300 cm^{-1} range. They are attributed respectively to the in-plane deformation δ_{OH} (520 cm^{-1}), to the out-of plane deformation vibration γ_{OH} (345 cm^{-1}) and to the Ni–O stretching vibration ν_{NiO} (460 cm^{-1}) [21].

Absorption bands related to adsorbed species are also often observed. Thus, a broad band centered at 3450 cm^{-1} and a weak absorption around 1630 cm^{-1} can be attributed to the respective stretching and bending modes of adsorbed water molecules. Similarly, IR spectra often display absorption bands due to nickel co-anions of the mother solution. For instance, adsorbed NO_3^- and CO_3^{2-} ions give rise to several bands in the range 1600 - 1000 cm^{-1} [13, 34(a)].

By contrast, Raman spectra have never been exhaustively analysed.

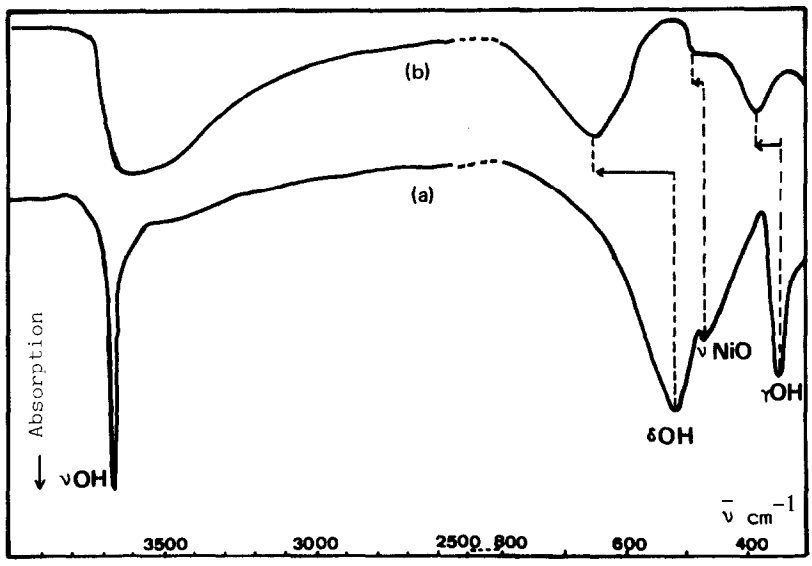

Fig. 2. Infrared spectra. (a) β-$Ni(OH)_2$; (b) turbostratic $Ni(OH)_2$.

2. Hydrous, imperfectly ordered Ni(II) hydroxides

Hydrated "α-type" Ni(II) hydroxides can be obtained either by chemical precipitation or by cathodic deposition upon electrolysis of a nickel salt solution. Nickel nitrate solutions seem to be particularly suitable as starting nickel solutions [1, 24 - 26], strong alkali or ammonia [14, 25, 26] being used as precipitating agents. In fact, a great variety of "α" hydroxides can be obtained, ranging from the hydrated turbostratic hydroxide proposed by Le Bihan [25] to a whole set of compounds for which it seems unrealistic to establish a clear frontier between hydroxides and hydroxy-salts, since they all represent unstable and non-stoichiometric intermediate compounds in the formation process of the more stable β-$Ni(OH)_2$ form.

Louër, for instance, who devoted many studies to nickel hydroxy-nitrates [27(a)], advocates the idea that "α hydroxides" commonly prepared by electrochemists [29 - 31] from nitrate baths might well be regarded as highly hydrated, degenerate forms of Ni(II) hydroxy-nitrates. The variations in crystallinity of the hydroxide samples thus obtained can be illustrated by the X-ray diffraction patterns of Fig. 3, which show a highly divided crystalline structure (Fig. 3(a)), microcrystalline solids (Fig. 3(b)) or turbostratic layered structures (Fig. 3(c)) [14, 25].

X-ray diffraction and crystalline structure

A detailed description of the imperfect crystalline organization of α-nickel hydroxide has been derived from X-ray diffraction spectra similar to those of Fig. 3(c). By comparison with the spectra of well crystallized β-$Ni(OH)_2$ (Fig. 3(d)) the major characteristics of spectra 3(c) are:

(i) the existence of intensity maxima around 8.5 and 4.25 Å instead of the (001) line at 4.6 Å;

(ii) the occurrence of asymmetric bands instead of the *hk*0 lines of the brucite structure;

(3) the vanishing of the general *hkl* lines of the brucite structure.

To account for this type of spectra Bode *et al.* [1] proposed a structure where the (001) layers of the brucite structure were still stacked up along the *c* axis but were separated by intercalar water molecules. They assumed a quasi-compact stacking of OH–H_2O–OH planes, and they assigned a fixed definite position for intercalar water molecules which would correspond to the idealized formula $3Ni(OH)_2 \cdot 2H_2O$.

Such a well-organized structure has, however, been rejected by both Le Bihan [25, 32] and McEwen [28] who proposed, instead, a turbostratic structure similar to those observed with some layered minerals and carbon black. The turbostratic nickel hydroxide consists of parallel and equidistant $Ni(OH)_2$ layers, similar to those found in β-$Ni(OH)_2$ (as evidenced by magnetic measurements [15 - 17]), but which are randomly oriented and separated by intercalar water molecules bonded to the hydroxyl groups by hydrogen bonds.

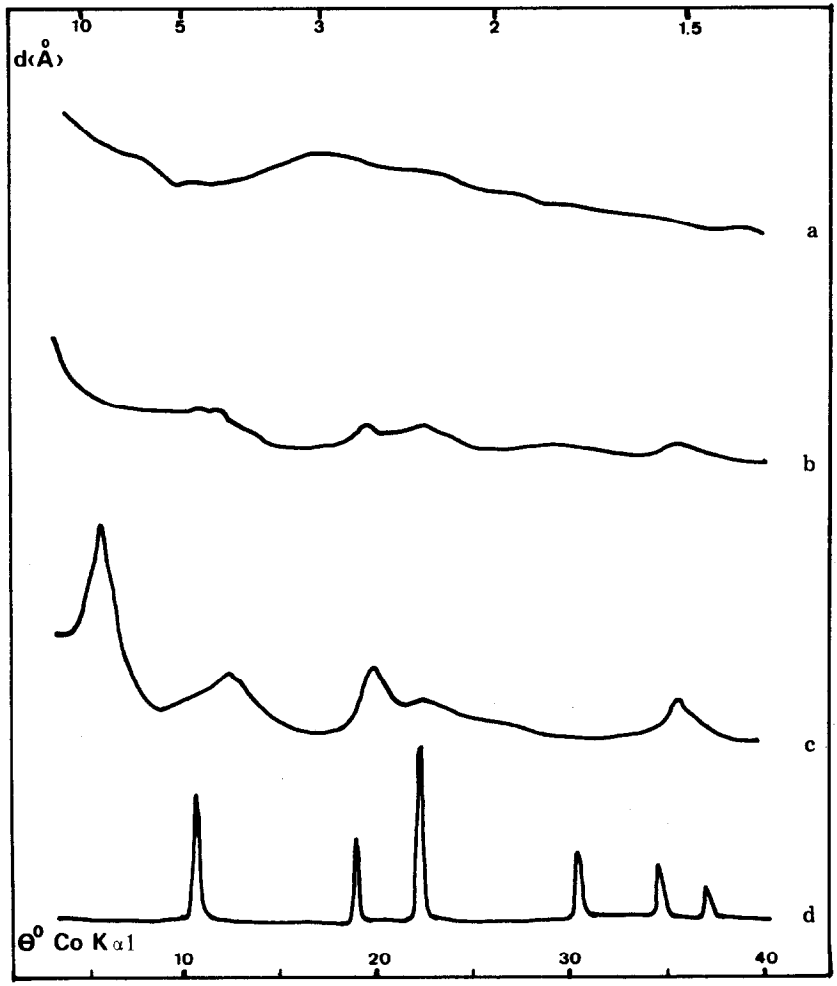

Fig. 3. X-ray diffraction spectra. a, Quasi amorphous nickel hydroxide precipitated by ammonia and washed by decantation; b, microcrystalline nickel hydroxide precipitated by NaOH; c, turbostratic nickel hydroxide precipitated by ammonia and washed by centrifugation; d, pure β-$Ni(OH)_2$ obtained by hydrothermal growth from an aqueous suspension of turbostratic hydroxide.

The lines around 8.5 and 4.25 Å displayed on the X-ray spectra are the first and second order diffraction maxima corresponding to the regular stacking of $Ni(OH)_2$ layers along the *c* axis.

The asymmetric *hk*0 bands are explained by the randomisation of the layers, *c* remaining constant. In his model McEwen assumes a very large delocalization of water molecules in the intercalar layer. Le Bihan [33] theorized a model assuming an hexagonal quasi-close-packed arrangement of intercalar water molecules, and interpreted the randomisation of the layers

as arising from variations of the hydrogen bond length between intercalar H_2O molecules and OH ions of the layers. He found [25] that the crystallites of the turbostratic hydroxide had a mean size of 30 Å along [00.1], which would correspond to a stacking of 5 layers. The mean size of the crystallites in the perpendicular direction was evaluated as 80 Å.

By electron microscopy [33, 35] turbostratic nickel hydroxides appear as aggregates of thin crumpled sheets, without any definite shape (Fig. 4(a)). This is a characteristic feature which has also been observed with turbostratic clays. It is difficult to obtain microdiffraction patterns from a turbostratic nickel hydroxide sample because it is easily dehydrated by the electron beam. Nevertheless, it has been possible to observe diffraction rings corresponding to the asymmetric bands *hk*0 observed by X-ray diffraction [33] (Fig. 4(b)).

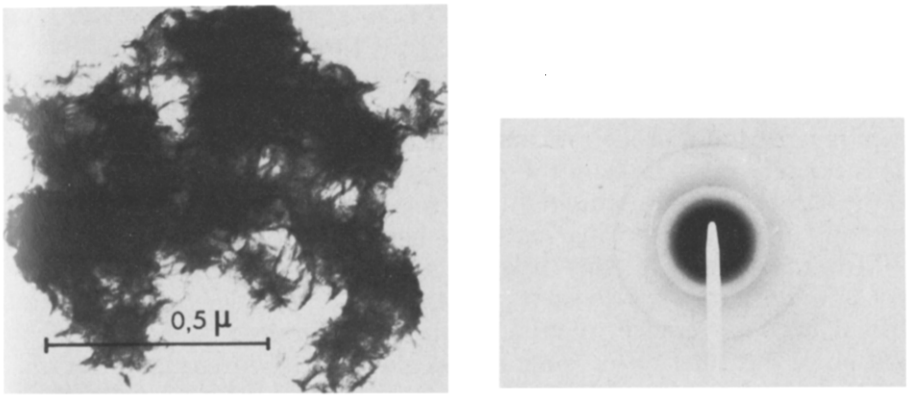

(a) (b)

Fig. 4. Turbostratic nickel hydroxide. (a) Electron microscopy; (b) selected area electron diffraction.

IR and Raman spectra

A detailed comparison of IR absorption bands for β-$Ni(OH)_2$ and α-$Ni(OH)_2$ has been undertaken by Le Bihan and Figlarz [33, 34(a)]. The sharp band at 3650 cm^{-1} corresponding to the stretching vibration ν_{OH} of β-$Ni(OH)_2$ is replaced by a broad and asymmetric band around 3500 cm^{-1} (Fig. 2), and the three bands corresponding to δ_{OH}, γ_{OH} and ν_{NiO} are shifted towards shorter wavelengths. In addition, the band at 1600 cm^{-1} corresponding to the angular deformation of molecular water appears more pronounced in the turbostratic hydroxide.

From these observations the authors concluded that the water molecules present in the turbostratic hydroxide were essentially in intercalar positions between the OH groups of the hydroxide layers and linked to these OH groups by hydrogen bonds. Such conclusions support those inferred from X-ray diffraction.

Turbostractic hydroxides also exhibit several bands in the range 1600 - 700 cm^{-1} which have been attributed to adsorbed nitrate and carbonate ions [33, 34(a)]. Due to the high degree of division of the turbostratic hydroxide the presence of adsorbed species cannot be avoided and is common to all hydrous, poorly crystallized nickel hydroxides.

In the case of electrochemically prepared "α" hydroxides, the presence of large quantities of nitrate ions (both adsorbed and intercalated) is confirmed unequivocally in Raman spectra [22].

Thermal stability

The thermal decomposition of nickel hydroxide with reference to the thermal decomposition of well-crystallized $Ni(OH)_2$ has been studied by Dennstedt [26] and Figlarz [34]. Finely divided β-$Ni(OH)_2$ loses adsorbed water below 160 °C. Hydrothermally grown β-$Ni(OH)_2$ with no adsorbed water does not exhibit this water loss and begins to dehydrate above 200 °C. By constrast α hydroxides (and particularly the turbostratic form) exhibit a weight loss of 30% below 150 °C, corresponding to water evolution. Most of this water is adsorbed water, but a part of it undoubtedly comes from the intercalar layers of the turbostratic structure.

This conclusion arises from the fact that after a thermal treatment at 150 °C the turbostratic structure is still observed by X-ray diffraction and IR spectroscopy, but the interplanar distance between two $Ni(OH)_2$ layers is lowered from 8.5 Å to 7 Å. This variation is fully reversible by rehydration [34(b)], and thermoanalysis suggests that the ~7 Å stacked structure would correspond to the presence of monomolecular intersheet water layers. Elimination of these intercalar water molecules and dehydroxylation of the hydroxide sheets then proceed in one single step for temperatures slightly higher than 200 °C, *i.e.*, in the same temperature range as β-$Ni(OH)_2$. This confirms that intercalar water molecules of the turbostratic structure are hydrogen bonded to OH groups.

NMR and impedance measurements [23] support thermal decomposition results. First, ^1H NMR studies show unequivocally the existence of two types of protons:

— one, associated with a broad absorption line, remains unchanged when temperature is increased; it corresponds to Ni(II) hydroxyl ions or to "bonded" intersheet water.

— the other, a narrow absorption line, disappears with increasing temperature and corresponds to adsorbed or "mobile" intersheet water.

Furthermore, whereas the conductivity of turbostratic hydroxides is around 10^{-5} Ω^{-1} cm^{-1} at room temperature, it falls to below 10^{-9} Ω^{-1} cm^{-1} (at the same temperature) once samples have been heated at 100 °C or dehydrated under high vacuum.

The transformation of "α" nickel hydroxides into β-$Ni(OH)_2$

The $\alpha \rightarrow \beta$ recrystallization reaction in water can be compared with the complex structural evolution of nickel hydroxy-salts upon either ageing in

their mother solutions [8] or hydrolysis [27(a)].

The crystal growth of microcrystalline nickel hydroxide has also been investigated by Bagno and Longuet-Escard [10], who described their primary hydroxide particles as hexagonal thin plates (thickness 10 Å, size 100 Å) and studied the ageing of these primary particles in the mother solution. Crystal growth would proceed by joining of the primary particles.

Le Bihan [35] proposed a different mechanism to explain the transformation of a turbostratic nickel hydroxide into β-$Ni(OH)_2$ in pure water. X-ray diffraction, IR spectroscopy, electron microscopy and selected area diffraction studies on the intermediary products support the hypothesis that the slow, room temperature transformation proceeds by a biphasic mechanism. The turbostratic hydroxide seems to dissolve slowly in water and β-$Ni(OH)_2$ appears by nucleation and growth from the solution.

Discussion — nickel hydroxides and NOE

The difficulty of obtaining well-crystallized β-$Ni(OH)_2$ by direct precipitation explains why β-$Ni(OH)_2$ currently used in pocket plates or in sintered plates cannot but exhibit structural and textural defects. This lack of perfection in crystallization must however be taken as the *sine qua non* reason for $Ni(OH)_2$ electroactivity. Unfortunately, to our knowledge, no correlation has ever been drawn between crystallization advancement and electroactivity, although studies such as Louër's X-ray diffraction line profile analyses on both hydroxy-salts [27(a)] and nickel hydroxides [27(b)] might provide a useful tool for such an investigation.

As for α-$Ni(OH)_2$, even if many battery manufacturers have seriously worked on the project (essentially by cathodic deposition), it has never been really exploited industrially. Depending on both the electrolytic bath and current densities, the phases obtained exhibit various salt contents and various inter-layer distances. On the other hand, chemically prepared α phases can be structurally controlled with more accuracy, but it becomes difficult to follow their evolution once extra water may enter and leave the intersheet space as soon as α-$Ni(OH)_2$ is in contact with the electrolyte. Therefore, in contrast with definite close-packed and turbostratic hydroxides studied in this section, neither "α" nor "β" hydroxides used by electrochemists can be considered as well-defined materials. This explains why results obtained on NOE are usually presented over a range of values.

B. Hydroxides and oxy-hydroxides with a nickel oxidation state higher than II

Although higher oxy-hydroxides have been as extensively investigated as Ni(II) hydroxides, there still exist various controversies about their structural characterization, their oxidation state, and the similarity of phases obtained through either chemical or electrochemical oxidation. However, in

an attempt to simplify their description, only two basic types of layered oxyhydroxides, differing by their interlamellar distance, are usually considered and are conventionally written β-NiOOH and γ-NiOOH.

While β-NiOOH is a relatively well defined material, γ-NiOOH represents a whole family of compounds exhibiting a large inter-sheet distance, of general formula $A_xH_y(H_2O)_zNiO_2$ (x, $y \leqslant 1$). A represents alkali ions (mainly K^+ and Na^+), and water molecules are intercalated between the NiO_2 slabs. The oxidation state of nickel lies within the range 3 - 3.75. The difficulty of characterizing such compounds is increased by the high degree of division they usually exhibit and by disordered sheet stackings, which result in a wide range of diffraction patterns.

In order not to present an extended list of all possible stoichiometric and textural variations, we shall concentrate on what can be considered as well established crystallographic grounds, bearing in mind that the purpose is to propose the clearest possible approach to NOE mechanistic paths.

γ and β materials can be obtained through either chemical or electrochemical reactions; chemical processes only will be considered in this section.

Preparations and structures

β-NiOOH

This compound was first studied by Glemser and Einerhand [36], who synthesized it by oxidation of nickel nitrate with $K_2S_2O_8$ in a 1N KOH solution at room temperature.

β-NiOOH crystallizes in the hexagonal system (a = 2.82 Å, c = 4.85 Å) and can be regarded as deriving from β-$Ni(OH)_2$ by a direct reaction removing one proton and one electron.

As in the case of oxides [37] the structure can be described as NiO_2 sheets of edge-sharing NiO_6 octahedra, protons being intercalated between the slabs, and oxygen atoms forming a hexagonal (AB) close-packing (*idem* β-$Ni(OH)_2$). It is noticeable that the a parameter, which corresponds to the Ni–Ni distance within the sheets, is significantly lower in NiOOH than in the case of $Ni(OH)_2$: 2.82 Å *vs.* 3.12 Å. On the other hand, the increase in the c parameter (inter-sheet distance), 4.85 Å *vs.* 4.60 Å, results from the enhancement of the repulsion between oxygen layers of adjacent NiO_2 sheets once protons are removed.

In constrast to β-$Ni(OH)_2$ [34(a), 38], IR spectra indicate that NiOOH is a hydrogen-bonded structure containing no free hydroxyl groups [38], and Kober's $^1_1H \rightleftarrows {}^2_1D$ exchange reaction tests on β-$Ni(OH)_2$ and β-NiOOH confirm [39] that protons are considerably more tightly bonded in the higher oxide than in the divalent one.

γ-NiOOH

The "γ" denomination was first given by Glemser [36] to a compound exhibiting a large intersheet distance and a high oxidation state obtained by

hydrolysis of the products derived from melting of NaOH and Na_2O_2 in a Ni crucible. Glemser's γ-NiOOH crystallized in the rhombohedral system, with corresponding hexagonal parameters a = 2.82 Å and c = 20.65 Å.

Years later, Bode similarly prepared "γ type" oxyhydroxides by solid state hydrolysis of $NaNiO_2$ in NaOH + Br_2 solutions [40]. In particular, he obtained a phase of compositon $Na_{0.32}H_{0.22}(H_2O)_{0.25}NiO_2$, corresponding to a mean oxidation state of nickel equal to 3.46.

The repetition of the same procedure on a single crystal of $NaNiO_2$ allowed Bode *et al.* [41] to obtain a single monoclinic crystal of $Na_{0.33}(H_2O)_{0.67}NiO_2$, with parameters a = 4.90 Å, b = 2.83 Å, c = 7.17 Å, β = 103.1°. The distortion from the ideal rhombohedral cell was small, and the pseudo-hexagonal parameters (a = 2.83 Å, c = 20.95 Å) are close to those given by Glemser for γ-NiOOH [36]. In fact, depending on the experimental conditions, a whole family of compounds having roughly similar X-ray diffraction patterns, but oxidation states of nickel ranging from 3.3 to 3.75, and different water and alkali cation contents within the sheets, can be obtained. Bode called such phases "γ_1" as opposed to the "γ_2" obtained from direct oxidation (NaOH + Br_2) of either $Ni(NO_3)_2$ solutions or α-Ni(II) hydroxides.

Basically, γ_1 and γ_2 oxy-hydroxides belong to the same structural family but exhibit different degrees of crystallinity, due essentially to different synthesis routes. While γ_1 phases are prepared from highly organized sodium nickelate through a direct reaction which allows all 3 elementary reactions (oxidation, cation exchange, water intercalation) to proceed simultaneously, γ_2 phases are obtained at room temperature either from Ni^{2+} solutions or from poorly crystallized α-$Ni(OH)_2$.

Two highly oxidized potassium nickelates, $K_{0.23}NiO_{1.8}$ and $K_{0.14}NiO_2$, have also been prepared by Bityutskii [42] through oxidation of $Ni(OH)_2$ by bromine at 170 °C in concentrated KOH; their hexagonal cell parameters are given in Table 1. These authors have also obtained the sodium nickelate $Na_{0.20}Ni_{1.8}$ having the same structure as $K_{0.23}NiO_{1.8}$ [42].

TABLE 1

Cell parameters of "γ-type" compounds

	a (Å)	c (Å)
$K_{0.23}NiO_{1.8} \cdot zH_2O$	2.82	21.15
$K_{0.23}NiO_{1.8}$	2.82	19.12
$K_{0.14}NiO_2 \cdot zH_2O$	2.82	21.15
$K_{0.14}NiO_2$	2.82	19.15
"γ-NiOOH" [36]	2.82	20.65

Crystallographic discussion

All reported γ-NiOOH phases correspond to layer structures and rhombohedral cells, which can be described as NiO_2 sheets having an octahedral nickel ion environment.

K^+ and Na^+ ions, protons, and water molecules are intercalated between the slabs.

It is interesting to relate this result to the numerous studies which have been devoted to anhydrous alkali layer oxides A_xMO_2 [37, 43, 44], and which show that in the rhombohedral symmetry only two types of oxygen packing can be found: ABCABC or ABBCCA. While in the former, alkali ions are inserted in octahedral environments, in the latter alkali ions exhibit a trigonal prismatic surrounding (Fig. 5). Bityutskii found an octahedral environment for potassium in $K_{0.23}NiO_{1.8}$ and a trigonal prismatic one for $K_{0.14}NiO_2$, and indicated that the diffraction patterns of $K_{0.14}NiO_2$ and γ-NiOOH are very close.

In addition, the crystal structure determination of $Na_{0.33}(H_2O)_{0.67}NiO_2$ has undoubtedly led to the assumption of an ABBCCA oxygen packing for the atoms belonging to the NiO_2 slabs [41]; Na^+ ions and oxygen atoms belonging to water molecules are in trigonal prisms. Braconnier and Delmas found that the X-ray diffraction pattern of γ-NiOOH obtained by hydrolysis of $NaNiO_2$ is very similar to those recorded for anhydrous alkali layer oxides (A_xMO_2) exhibiting an ABBCCA oxygen packing [45]. Thus all the available data seem to corroborate the hypothesis of an ABBCCA oxygen packing for γ-NiOOH.

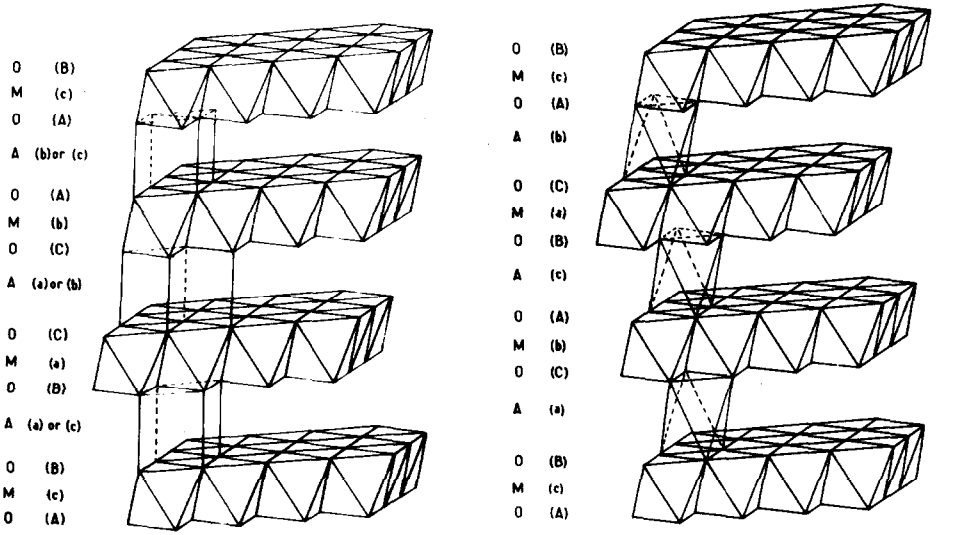

Fig. 5. Structure of layer oxides with rhombohedral lattices. ABCABC and ABBCCA oxygen packings.

The overall redox reaction β-$Ni(OH)_2 \rightarrow \gamma$-NiOOH which is obse under strong oxidation conditions in an electrochemical cell thus suppc transition from the AB oxygen packing of β-$Ni(OH)_2$ to the ABBCC/ oxygen packing of γ-NiOOH. Upon oxidation of β-$Ni(OH)_2$, β-NiOOI which has the same AB packing, is first obtained. Further oxidation to NiOOH implies that electrons are removed from Ni^{3+} ions (giving Ni^{4+}) protons from the intersheet space. At the same time water is intercalat protons are exchanged by alkali ions, and a sheet glide occurs, which is trated in Fig. 6. In consequence of this structural rearrangement the int sheet distance increases (c β-NiOOH = 4.85 Å $\rightarrow$ $c/3$ γ-NiOOH $\geqslant$ 7 Å). ' minimum difference in the intersheet distance between both phases coi sponds approximately to the size of a water molecule [28].

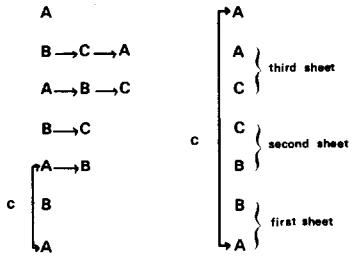

Fig. 6. Transition between AB and ABBCCA oxygen packing by gliding of the seco third sheets.

C. Structural approach of the NOE behaviour

The transitions which can take place in the nickel electrode can summarized, as previously shown by the Bode diagram: (1), (2) (3).

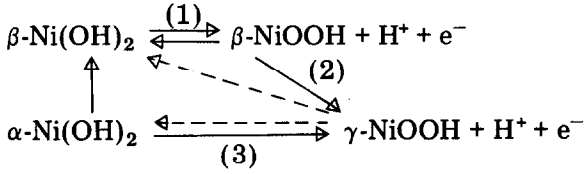

Reactions (1), (2) and (3) can now be discussed on a strictly structural

(a) Cycling between β-$Ni(OH)_2$ and β-NiOOH

The NOE can be cycled between these two phases by avoiding ov charge. To illustrate the involved topochemical mechanism the redox r tion can be written:

$$\beta\text{-}H_2NiO_2 \rightleftarrows \beta\text{-}H_{2-x}NiO_2 + xH^+ + xe^-.$$

Several studies have been carried out in order to determine whether th tion is homogeneous or heterogeneous. X-ray diffraction studies sugges

the reaction is heterogeneous. Only β-$Ni(OH)_2$ and β-NiOOH are apparently present during charge or discharge and no continuous variation of cell parameters between both limits is observed [44]. Kober's IR analyses support this hypothesis; that is, there is no shift of the vibration frequency of the OH groups upon oxidation, and the IR spectrum of β-NiOOH appears continuously during the charge [38].

Barnard's investigation of the potential evolution of the nickel electrode during charge indicates a variation of the potential between states 2 and 2.25, while it remains constant for oxidation states higher than 2.25. This suggests that the reaction would be homogeneous between 2 and 2.25 with a material closely related to β-$Ni(OH)_2$. For further oxidation the reaction would then be heterogeneous, in close agreement with X-ray and IR data. However, direct determination of the oxidation state of the coexisting phases proves extremely difficult because of either O_2 evolution or the formation of a small amount of γ phase [46], though X-ray and IR studies tend to indicate that stoichiometries are relatively close to H_2NiO_2 and $HNiO_2$, respectively [36, 38, 47]. In consequence, it should be noted that the intermediate phase $H_{1.33}NiO_2[Ni_3O_4(OH)_4]$ suggested by several groups of workers [36, 48] has never been observed during the electrochemical process [44].

(b) Oxidation of β-NiOOH and α-$Ni(OH)_2$ to γ-NiOOH

High charge rates and prolonged overcharge of β-$Ni(OH)_2$ in KOH, as well as the ageing of β-NiOOH, favour the formation of γ-NiOOH.

To account for the lower discharge potential of γ-NiOOH with respect to β-NiOOH [46, 49, 50], it may be of interest to compare this result with those obtained with A_xMO_2 layer oxides. Recent studies have been done on A_xMO_2 phases (M = 3d elements) used as cathodes in electrochemical cells of the type: $A/AClO_4$ + propylene carbonate/A_xMO_2 (A = Li, Na), [51, 52]. The potentials of such cells depend obviously on the nature of M and on the intercalation ratio x. But the most important parameter influencing the potential is the nature of the alkali ion.

Due to the ionic character of the M–O bonds, non-stoichiometric layer oxides are very unstable. The repulsions between adjacent oxygen layers are very important and the A_xMO_2 phase stability varies with the intersheet distance, *i.e.*, the alkali radius.

Considering two cathodes differing by the nature of the alkali ion, the smaller potential is observed (at the same oxidation state of M) for that with the largest alkali ion.

On charge, the potential increases to the upper value fixed by the stability of the electrolyte. This means that a cathode with a large intersheet distance will reach higher oxidation levels than one with a small intersheet distance [53].

Such results can be transposed to the case of nickel hydroxides. The greater intersheet distance of γ-NiOOH with respect to β-NiOOH ($\geqslant$7 Å *vs.* 4.85 Å) results in a smaller equilibrium potential and a larger capacity.

Inevitably, this raises the question of why γ-NiOOH does not form directly from β-$Ni(OH)_2$ upon oxidation. It can reasonably be assumed that it is mainly a matter of kinetics and steric hindrance. While the oxidation of β-$Ni(OH)_2$ to β-NiOOH only implies the removal of one proton and one electron, with no other structural change except a slight cell parameter variation, the oxidation to γ-NiOOH requires the intercalation of H_2O molecules, the exchange of protons and alkali ions, and a sheet glide. As a consequence a higher energy barrier exists and β-NiOOH is first obtained, γ phases appearing ultimately upon overcharge or ageing in KOH.

This reaction scheme is corroborated by the fact that γ-type oxy-hydroxides are formed directly from α-$Ni(OH)_2$ since, in this case, the intersheet distance is already expanded and there is no need to intercalate additional water.

D. Thermodynamic and kinetic approach of the NOE behaviour

1. Thermodynamic properties

Since the pioneering work of Conway [54] who first established that the potential of charged nickel hydroxide electrodes is well above the reversible oxygen potential, and who derived (from e.m.f. decay measurements) the first trustworthy results concerning the thermodynamic properties of Ni hydroxides, considerable progress has been achieved in the field.

Reversible potentials have been measured for β^{II}/β^{III} and α/γ systems over a wide range of KOH concentrations and for various states of charge. Ageing of nickel hydroxide electrodes has also given rise to a number of recent papers by Bramham [56], Prikryl [57] and Barnard [24].

1(a). Reversible potentials of the β^{II}/β^{III} and α/γ systems

Both β^{II}/β^{III} and α/γ systems in their "activated" and "deactivated" forms have been exhaustively investigated by Barnard [55] who also established the influence of KOH and H_2O activities on the reversible potentials.

To mention the "activated" forms only, he derived the equations

$$\alpha \rightarrow E_R^{\alpha} = 0.3919 - 0.0139 \log a_{KOH} + 0.0386 \log a_{H_2O}$$

(w.r.t. Hg/HgO/KOH),

$$\beta \rightarrow E_R^{\beta} = 0.4428 - 0.0028 \log a_{KOH} + 0.0315 \log a_{H_2O},$$

but an important contribution of his work was to establish that both α and β systems can exist in a wide variety of forms associated, respectively, with the potential ranges 0.392 - 0.440 V and 0.443 - 0.470 V, which confirms electrochemically the great variations observed in the structure and the texture of both systems.

As seen above, it was found that those potentials were independent of the degree of oxidation of the nickel cation over an appreciable range of

oxidation states, which supports, in both cases, the hypothesis of a heterogeneous reaction.

One major difficulty in studying such systems is obviously the interference of oxygen evolution both on charge and self-discharge.

Conway and Bourgault [54] were the first to tackle the problem of self-discharge. They proposed a scheme of two consecutive processes,

$$M + OH^- \rightarrow MOH + e^-$$

$$MOH + OH^- \rightarrow MO + H_2O + e^-$$

$$MO + MOH \rightarrow MHO_2 + M \quad (\text{or } MO + OH^- \rightarrow MHO_2 + e^-)$$

$$MHO_2 + MOH \rightarrow 2M + H_2O + O_2$$

(M refers to the surface oxides), to account for experimental evidence that the rate controlling process in self-discharge of the nickel oxide electrode is the anodic partial reaction of oxygen evolution.

From potentiodynamic investigations, however, Paszkiewicz [58] noticed that it was not until the electrode had stayed on open circuit for 24 h that its capacity decreased. By contrast, the electrode capacity increased in the first hours following the charge and a potential decrease was observed. This could be interpreted in terms of equalization of proton concentration in the solid phase, with subsequent reduction of the most oxidized surface oxides and increase of the oxidation state of the bulk oxyhydroxides (together with possible structural rearrangements, as we have seen before).

The mechanism of oxygen evolution on overcharge has also been widely investigated, particularly on thin oxide films [59 - 62] to minimize mass transfer effects through the bulk hydroxides. For instance, Bronoel's mechanistic approach [61] led him to assume a first step of OH^- discharge followed by a chemical recombination of OH_{ads} and OH^- ions to give O^-_{ads} which is then oxidized. The assumed mechanism takes account of the variation of the current as a function of the OH^- activity in solution and of the existence of two Tafel regions in the log $i = f(\eta)$ curves.

1(b). Electrode ageing

At least four major causes can account for the observed evolution performance of nickel hydroxide electrodes upon ageing:

(a) the chemical transformation α-$Ni(OH)_2 \rightarrow \beta$-$Ni(OH)_2$;

(b) the active mass textural evolution due to the lattice modifications arising from the sequential redox processes β-$Ni(OH)_2 \rightarrow \beta$-NiOOH $\rightarrow$ γ-NiOOH;

(c) entropic order–disorder phenomena associated with metastable states created by heterogeneous phase reactions;

(d) the structural and stoichiometric perturbations induced by the introduction of alkaline ions in the active mass.

(a) The $\alpha \rightarrow \beta$ transformation, already studied in Part A (chemical evolution) has been followed by voltammetric sweeps by McArthur [63], Arvia [64], and Barnard [24]. McArthur and Arvia attributed the replacement of

the anodic peak at 0.390 V by a peak at 0.460 V to the direct transformation $\alpha \rightarrow \beta^{II}$. Barnard, on the other hand, advocated that α-$Ni(OH)_2$ first transforms, by a first order reaction, into a "deactivated" α phase which shows the β-type diffraction pattern but has the same marked dependence of oxidation/reduction potentials on alkali and water activity as the α phase, and leads to γ-NiOOH as the oxidation product.

The final transformation of α to β occurs after a time or a number of cycles which depends on the initial way of precipitation of the α phases, electrochemically precipitated phases being much more stable than chemically precipitated phases.

(b) The transformation on cycling of electrochemically precipitated α phases has been followed by voltammetric sweeps in a range of KOH concentrations [65]. In the absence of overcharge, the charge/discharge reactions change from the α/γ system to the β-$Ni(OH)_2$/NiOOH system. The reaction takes place in two steps (Fig. 7):

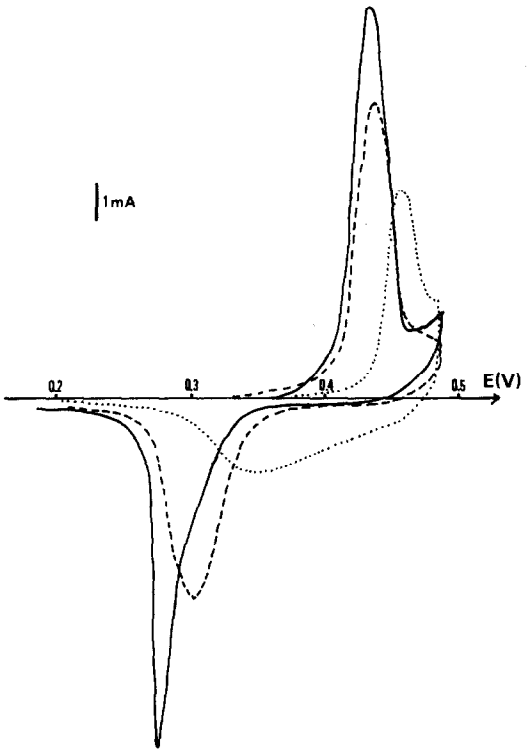

Fig. 7. Evolution from the α/γ to the β^{II}/β^{III} system. Voltammetric sweeps of electrochemically precipitated α phases in a sintered nickel electrode. 8N KOH; potential sweep 0.1 mV s^{-1}; Ref. Hg/HgO. Curve 1 ——: cycle 1, α/γ system; curve 2 — — —: cycle 3, β phase with low charge/discharge potentials; curve 3 · · ·: cycle 65, typical β phase.

(i) Change from the α/γ system (curve 1) to a phase system with peak shape characteristics of β phases but lower charge and discharge potentials (curve 2). This step could be identified with the production of Barnard's [24] "deactivated" α phase in the discharged state. It may be added that the same phenomenon exists in the charged condition.

(ii) Progressive increase of the charge/discharge potentials with corresponding decrease of the chargeability (curve 3). This second step is a slow one, and the charge potential finally remains lower than that reached upon cycling with chemically precipitated β-$Ni(OH)_2$. This transformation can be associated with point (c).

(c) Order/disorder phenomena in the β-$Ni(OH)_2$/NiOOH system, which have been studied voltammetrically on chemically precipitated hydroxides. Depending on ageing, state of charge, and rate of charge, the discharge potential of the phase may vary over a range of 40 mV (*cf.* Fig. 8).

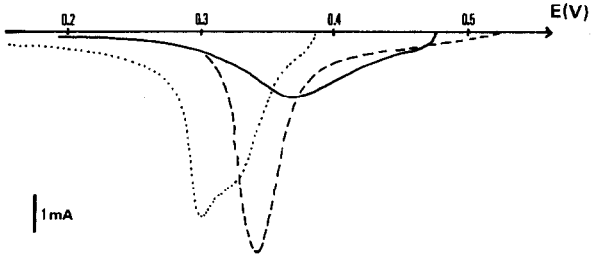

Fig. 8. Influence of the state of charge on the discharge potential of β NOE; cathodic voltammetric sweeps are recorded after galvanostatic charges at the $C/5$ rate in 5.2N KOH. ——: 3h charge; — — —: 7 h charge; · · ·: peaks of β^{III} and γ obtained after prolonged ageing. (Potential sweep 0.1 mV s^{-1}; ref. Hg/HgO.)

2. Electrochemical mechanisms and kinetics

E–Log *i* investigations for the nickel hydroxide electrode reveal complex features for which there are not yet any completely satisfactory explanations. However, it seems that the reaction kinetics in the solid phase are certainly responsible for composition differences between the bulk hydroxide and the surface.

The best documented approach, based on thermodynamic considerations, is that of Barnard [55], which applies the thermodynamics of mixing to account for the independence of the discharge potential of the NOE as a function of nickel oxidation state. Constant potential regions could then derive from heterogeneous equilibria between pairs of co-existing phases, both containing nickel in upper and lower states of oxidation. However, such a model remains essentially macroscopic and most electrochemists are more interested in investigations of charge transport associated with the solid state process of the overall reaction:

$$Ni(OH)_2 + xOH^- \rightleftharpoons NiO_2H_{2-x} + xe^- + xH_2O.$$

Three main approaches have been developed and tested (mainly on α hydroxides):

(a) McArthur [63] assumed that the charge-transfer was reversible and that the reaction rate was controlled by proton diffusion. Linear sweep techniques and potentiostatic pulses on α-$Ni(OH)_2$ electrodes led him to propose diffusion coefficients varying from 2×10^{-9} cm^{-2} s^{-1} to 4.6×10^{-11} cm^{-2} s^{-1} and an activation energy of about 2.2 kcal-deg^{-1} mol^{-1} in the temperature range 25 - 70 °C. Similar results were obtained by Tysyachnyi [66] on thin α films, assuming a single phase model, and by Briggs [67].

(b) Takehara [68] considered that the rate determining step of the reaction was the diffusion process of protons and/or defects in the hydroxide layer. However, his model was based on the hypothesis of a variable surface concentration of proton sites and vacancies set at the electrolyte interface by the charge-transfer reaction. He supported his model with both potential decay and electrode impedance measurements and derived diffusion coefficients which are quite similar to those obtained by McArthur.

(c) Feuillade [69], by contrast, claimed that anion (OH^-) transfer was predominant over proton transfer in the oxidation of electrodeposited nickel hydroxide. He deduced such conclusions from ^{16}O - ^{18}O and ^{1}H - ^{3}H isotopic exchange measurements which made it possible to calculate anionic exchange currents of 60 $\mu A/cm^2$ and 40 $\mu A/cm^2$ for Ni(II) and Ni(III) hydroxides, respectively.

Though direct OH^- mobility and exchange may seem improbable in the (supposedly) topochemical reaction β-$Ni(OH)_2 \rightleftarrows \beta$-NiOOH + H^+ + e^-, the hypothesis of oxygen exchange in the α/γ system is worthy of consideration, as this phenomenon is certainly plausible. Thus, Feuillade's best contribution may have been to establish the possibility of a dual type of transport (H^+ and OH^-/H_2O) in the solid phase, the relative importance of both types of transport depending most probably on the interlayer distance and the subsequent presence of "free" or "bound" water. It must be pointed out that, from a kinetic point of view, the α/γ redox transfer appears more rapid than the β^{II}/β^{III} transfer. If we assume that proton mobility is the rate determining step in the β^{II}/β^{III} reaction, the kinetics difference stresses the importance of interlayer water as a charge transport factor in the α/γ system.

In fact, a major weakness of all these models lies in the general implicit assumption that a constant mechanistic path prevails all along the redox process. This is undoubtedly a rough approximation if we accept the idea that the NOE behaviour involves more than two oxidation states. Indeed, both Labat's [70] magnetic measurements and Aleshkevich's [71] or Dibrov's [72] theoretical energy considerations would tend to confirm the hypothesis that divalent nickel is directly converted to tetravalent nickel (which then reacts in the solid phase), and that relatively stable high-valency states of nickel can exist in charged electrodes [73].

This raises the long debated arguments on NOE faradaic behaviour:

(i) maximum state of oxidation in the bulk?

(ii) role of the electrolyte concentration?
(iii) role of the cations?
(iv) cause of residual capacity?

One point is now well established about nickel hydroxide electrodes: on cycling, electrodes do not revert to the Ni(II) state. An average oxidation state of 2.3 is generally accepted in the literature and is interpreted as the basic level of Ni(III, IV) defects required to give the hydroxide bulk sufficient electronic conductivity and defect homogeneity. β-$Ni(OH)_2$ has a very poor electronic conductivity due to the band structure of nickel in the divalent state and to the large intercation distance d_{Ni-Ni} = 3.12 Å. By contrast, the shorter Ni–Ni bonds (2.86 Å) of NiOOH favour a better orbital overlapping.

The second (low potential) plateau observed when forcing the active material to return to the divalent state is thus a non-equilibrium process that might be compared with the behaviour of a mixed *p.n.* semiconducting material under reverse bias conditions [49]. The well-known "forming process" of NOE is therefore related to the necessity to create enough stoichiometric and textural defects in the bulk hydroxide to ensure activation.

It is in connection with the oxidized states that most controversies exist, however, both on the structure of the compounds and on the validity of the oxidation values derived from either iodometric measurements of active oxygen or electrode faradaic capacities. However, experimental data undoubtedly show that α and β hydroxides exhibit different charging abilities and can reach various oxidation states, depending on structural and textural conditions as well as on charge characteristics (see Fig. 9, the influence of the electrolyte and of overcharge upon the capacity delivered by a β-$Ni(OH)_2$ electrode).

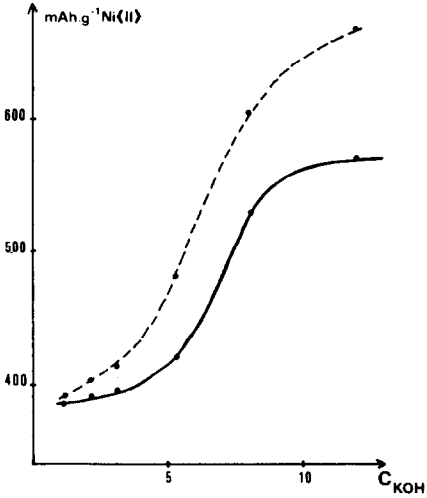

Fig. 9. Influence of the KOH concentration upon the capacity of β NOE. Discharges are run at the *C*/5 rate. ——: After 1.4 *C* overcharge (*C*/5 rate); — — —: after 4.8 *C* overcharge (*C*/10 rate).

More than 1 e^- can be exchanged in an apparently reversible way (thus involving at least a transition between states 2.3 and 3.3), and there is no reason to believe that the excess capacity comes from the reduction of oxygen or hydroperoxide molecules on the active material (*cf.* Section C). Nevertheless, neither IR analysis [38, 74], X-ray diffraction, nor DTA [75] have been able to provide clear conclusions on the ultimate oxidation states of nickel in NOE, part of the difficulty being the instability (evidenced by self-discharge) of the highest states obtained upon overcharge.

E. Role of the electrolyte on the NOE behaviour

The electrolyte plays an essential part in the NOE working. Since it is involved in the material transfer to and away from the electrodes by the exchange of both OH^- ions and alkali, it controls points as important as charge acceptance, charge and discharge potentials, structural changes, electrode ageing, ... Indeed, charge acceptance depends greatly on the oxygen evolution potential, and the characteristics of the electrode redox transfers can be largely affected by the possibility of alkali intercalation within the crystal lattice.

1. Oxygen evolution and charge acceptance

Rubin and Baboian [76] studied the electrochemical behaviour of nickel hydroxide in binary aqueous alkali hydroxides, $MOH–H_2O$ ($M^+ = Li^+$, Na^+, K^+, Rb^+,Cs^+) for the temperature range —40 - +60 °C (at concentrations corresponding to the maximum conductance), and observed maxima in the "capacity *vs.* temperature" curves for each electrolyte.

The best capacities are obtained with sodium and lithium electrolytes at temperatures higher than 30 °C, with potassium at intermediate temperatures, and with rubidium or cesium at low temperatures. Such results were explained as superimposed variations in electrode polarization and oxygen evolution with temperature, both variations being partly interpreted in terms of electrolyte interactions.

The oxygen evolution overpotential proves to be much more sensitive to changes in the concentration or the nature of the ionic electrolyte population than the Ni(II)/Ni(III, IV) system, and it is thus possible to optimize the chargeability of NOE for a whole range of temperatures (—40 - +50 °C). Hence, small quantities of lithium hydroxide have been added to standard KOH electrolytes almost since Edison's work, to shift the OER (Oxygen Evolution Reaction) to more positive potentials and improve charge acceptance. Kelson *et al.* [77] found that the use of lithiated electrolytes simultaneously lowers the nickel hydroxide oxidation potential, but that the increase of charge acceptance is partly compensated by the end of discharge at a higher oxidation level. Bonnaterre [78] gave further evidence that the use of lithiated electrolytes could increase the capacity of batteries up to 20%, but it also increased self-discharge.

2. Influence of the cations on the structure and the electrochemistry of the oxidized phases

Harivel [79] showed that the γ phases are easily obtained on overcharging in KOH and that their formation is promoted by the use of concentrated solutions.

Similar results are observed in NaOH, but γ phases (defined as layered compounds with intersheet distance $\geqslant 7$ Å) cannot be obtained in pure lithium hydroxide electrolytes, and divergent results have been published in the case of RbOH and CsOH [50, 80]. Such results underline the preeminent role played by the alkali cations in the whole redox process, through either their size, their acidity level, their stabilizing effect, etc.

The case of Li^+

Lithium nickelate is the only phase obtained upon oxidation in pure LiOH electrolytes. Penetration of Li^+ in the crystal lattice is interpreted as an exchange reaction between Li^+ and protons, and Guliamov [81] brought theoretical support to this hypothesis.

Lithium nickelate displays a low potential discharge peak and exhibits a poor reversibility, especially at low temperatures [82]. The discharge takes place through a homogeneous reaction within a single solid phase, as shown both on the X-ray diagrams (the structure of lithium nickelate remains apparent, and no $Ni(OH)_2$ is noticed until almost the end of discharge) and by the shape of the discharge curve [82]. Due to the absence of γ-phase, the capacities of the electrodes remain low in pure LiOH. Thus lithium must be used with extreme caution since, depending on experimental conditions, it can either improve or poison NOE operation. In KOH solutions containing lithium as an additive, capacity increases with the addition of LiOH up to an atomic ratio Li/Ni = 0.06, and decreases beyond this point. The maximum capacity is displaced towards higher values of the Li/Ni ratio with increasing temperatures [83]. At low Li^+ concentrations, β and γ phases are formed, whereas lithium nickelate is obtained at higher Li^+ contents.

All three phases have been obtained simultaneously in 7N KOH–1N LiOH upon moderate overcharge, and characterized by their three voltammetric peaks [65]. Lithium nickelate discharges at a potential 50 mV lower than the γ phase. Its formation proceeds with a decrease in the apparent degree of oxidation of nickel in the charged electrode [83] and an increase in the discharged electrode [74]. The rate of formation of lithium nickelate is also increased with the total OH^- concentration of the electrolyte.

The intersheet distance of lithium nickelate, $c/3 = 4.7$ Å with respect to hexagonal axes [84], is considerably smaller than that of γ-NiOOH, and the general observation (particularly true in the case of pocket plates) that the addition of LiOH to KOH improves NOE longevity may well find its origin in a mechanical swelling limitation. The beneficial effect of lithium against NOE poisoning by iron (or ferrate ions) can (all the same) be interpreted on the same basis, *i.e.*, the impossibility of large radius species penetrating the crystal lattice.

From an electronic point of view the beneficial effect of LiOH additions to KOH is frequently attributed to *p*-type semiconduction enhancement in the charged phase, as noted in lithium doped NiO (β-NiOOH being on the other hand an *n*-type semiconductor [85]), but a clear interpretation of the conduction process of such disordered systems does not seem to be at hand. However, Takehara [68] concluded from charge and discharge activation energy measurements that the diffusion rate of protons (and/or defects) in the crystal lattice was affected by the presence of Li^+ ions, thus showing a specific kinetic influence of lithium on the redox transfer.

F. The role of foreign metallic cations on the NOE behaviour

A review of NOE cannot fail to devote some lines to this important point. In fact, Harivel [86], Casey [87], Doran [88], and many others have studied the influence of numerous foreign cations on NOE: Ag(I), Co(II), Mn(II), Ba(II), Zn(II), Pb(II), Mg(II), Cd(II), Al(III), As(III), Sb(III), Bi(III), Mn(IV), Pb(IV), Si(IV), . . . The results have been either totally negative or selectively positive, with detrimental side effects on self discharge, faradaic behaviour, charge and discharge potentials, or durability. Cobalt and cadmium, however, because of their practical interest, deserve special attention.

Cobalt hydroxide, which can *syn*-crystallize in the same α and β forms as nickel hydroxide, is commonly used by sintered plates manufacturers to improve charge acceptance of nickel electrodes, particularly at high temperatures. Cobalt (Co/Ni = 2 - 5%) shifts the reversible potential of NOE some 20 - 40 mV cathodically and improves the electrode stability. Voltammograms [89] clearly indicate that the charging process occurs more reversibly in the presence of coprecipitated cobalt hydroxide than in its absence. Since charge transfer appears to be controlled primarily by mass transport through a solid in which the conductivity depends upon the state of charge it can be presumed that cobalt (which is certainly present in the oxidation state III) optimizes the lattice imperfections in the active material so that conductivity is substantially increased. However, large quantities of cobalt would tend to inhibit the NOE behaviour since cobalt hydroxide exhibits a low redox reversibility [3]. Similar overall results are also claimed for barium.

In the case of cadmium, Ness [90] and Cittanova [91] have shown that coprecipitation of cadmium hydroxide partially inhibits swelling and promotes the NOE initial activity. The presence of Cd^{2+} ions thus seems to act on the conductivity and maintain the cohesion of the NiO_2 slabs, while forbidding the introduction of water and alkali within the crystal lattice. The formation of γ phases is thus delayed; consequently the oxidation of nickel to states higher than III is made difficult, and there is a loss in charge acceptance.

Voltammograms obtained from electrodes containing coprecipitated nickel and cadmium hydroxides have confirmed these results [65].

Conclusion

If we review the principle ideas resulting from a consideration of this paper, we find that despite the recent gain of a deeper and closer insight into the NOE electrochemical behaviour through, for instance, the measurement of E_R potentials in different electrolytes, or the determination of the homogeneous or heterogeneous character of the redox process, a number of basic questions still remain partially or totally unanswered. In particular, it may seem surprising that in spite of the tremendous amount of experimental data accumulated over past years, we are unable to characterize charged and uncharged electrodes in a precise manner in the various possible electrolytes.

We have seen, however, that a strictly structural approach to the redox reaction can throw some light on the different redox routes, and particularly on the "γ" phenomenon, by relating it to better known solid state properties. It is reasonable to assume that, in the next few years, solid state electrochemistry will help to find answers to the main problems posed by the redox process and its interaction with the solvent, namely:

(i) The role of the electrolyte in the oxidation reaction: the importance of the cation in the structural changes is well known, but how does it take place?

(ii) Transport modes: how are these influenced by the respective populations of protons, OH^- ions and alkali ions?

(iii) Lithium, cobalt, barium . . .: how do they modify the conduction process?

(iv) Controversy over the γ phase(s): can the γ phase(s) be defined by a precise formula (an hypothesis supported recently by Barnard [80]), or at least can we propose definitions in better conformity with reality?

Finally, this paper, which results from close collaboration between solid state chemists and electrochemists, emphasizes two basic truths:

(a) As in any other chemical reaction, the redox reactions which occur in the NOE obey fundamental steric and stoichiometric laws. The complexity of all possible mechanisms, together with the existence of interfering reactions (such as oxygen evolution), have engendered a belief among electrochemists that NOE operation is not based on well defined reactional grounds. By contrast, we have stressed that, despite an apparent state of confusion on the nature and structure of all involved phases, general steric mechanisms could be derived from the available data.

(b) Electroactivity and electrochemical characteristics cannot be interpreted other than in close connection with structural and textural parameters. This justifies the importance that we have given in this paper to the early sections, to stress that there may exist as many structural and electrochemical differences within the same "α" or "β" family (*e.g.*, between a chemically prepared turbostratic hydroxide and an electrochemically deposited "α-type" hydroxy-nitrate) as between α and β hydroxides taken as generic entities.

A basic knowledge of the starting materials and of their chemical redox reactivity is thus essential to a better understanding of the NOE behaviour.

Acknowledgements

The authors thank Drs C. Fouassier and G. Feuillade for interesting discussions and helpful support.

References

1 H. Bode, K. Dehmelt and J. Witte, *Electrochim. Acta, 11* (1966) 1079.
2 P. C. Milner and U. B. Thomas, in C. W. Tobias (ed.), *Advances in Electrochemistry and Electrochemical Engineering*, Vol. 5, Interscience, New York, 1967, p. 1.
3 G. W. D. Briggs, Chem. Soc. Spec. Period. Rep., *Electrochemistry, 4* (1974) 33.
4(a) S. U. Falk and A. J. Salkind, *Alkaline Storage Batteries*, Wiley, New York, 1969.
(b) S. U. Falk, in M. Barak (ed.), *Electrochemical Power Sources*, IEE Publications, P. Peregrinus Ltd., 1980, p. 324.
5 A. J. Bard, *Encyclopedia of Electrochemistry of the Elements*, Dekker, New York, 1975, p. 349.
6 J. P. Hoare, *The Electrochemistry of Oxygen*, Interscience, New York, 1968.
7 H. R. Oswald and R. Asper, in R. M. A. Lieth (ed.), *Preparation and Crystal Growth of Materials with Layered Structures*, Reidel, Dordrecht, 1977, Ch. 3, p. 109.
8 W. Feitknecht and A. Collet, *Helv. Chim. Acta, 22* (1939) 1428; *23* (1940) 180.
9 A. Berger, *Kolloid Z., 103* (1943) 13; *104* (1944) 24.
10 D. Bagno and J. Longuet-Escard, *J. Chim. Phys., 51* (1954) 215.
11 E. Suoninen, T. Juntunen, H. Juslen and M. Pessa, *Acta Chem. Scand., 27* (1973) 2013.
12 A. Merlin and S. J. Teichner, *C.R. Acad. Sci., 236* (1953) 1892.
13 F. Fievet and M. Figlarz, *J. Catal., 39* (1975) 350.
14 F. Fievet, *Thèse Doctorat d'Etat*, Paris VII, 1980.
15 J. Deportes, P. Mollard, J. Penelon, S. Le Bihan and M. Figlarz, *C.R. Acad. Sci., Ser. B, 272* (1971) 449.
16 J. Deportes, *Thèse 3ème cycle*, Grenoble, 1971.
17 L. Neel, *Nuovo Cimento, 6-X, Suppl., 3* (1957) 942.
18 J. D. Bernal and H. D. Megaw, *Proc. R. Soc. London, Ser. A, 151* (1935) 384.
19 W. R. Busing and H. A. Lévy, *J. Chem. Phys., 26* (1957) 563.
20 S. S. Mitra, *Z. Kristall., Bd 116* (1961) 149; *Solid State Phys., 13* (1962) 1.
21 C. Cabannes-Ott, *Ann. Chim., 5* (1960) 905.
22 M. Couzi, F. Cruege and P. Oliva, unpublished results.
23 J. C. Brethous, J. J. Braconnier, G. Villeneuve and P. Oliva, unpublished results.
24 R. Barnard, C. F. Randell and F. L. Tye, *12th Int. Symp. Power Sources, Brighton, 1980*, Academic Press, London, 1981.
25 S. Le Bihan, J. Guenot and M. Figlarz, *C.R. Acad. Sci., Ser. C, 270* (1970) 2131.
26 W. Dennstedt and W. Löser, *Electrochim. Acta, 16* (1971) 429.
27 (a) D. Louër, M. Louër, D. Grandjean and A. Le Bail, *Acta Crystallogr., B 29* (1973) 1696, 1703, 1707; *Rev. Chim. Minér., 17* (1980) 522; *J. Solid State Chem., 13* (1975) 319.
(b) D. Louër, D. Weigel and J. I. Langford, *J. Appl. Crystallogr., 5* (1972) 353.
28 R. S. McEwen, *J. Phys. Chem., 75* (1971) 1782.
29 L. Kandler, *Brit. Pat. 917,291* (1963).

30 E. J. McHenry, *Electrochem. Technol., 5* (1967) 275.
31 R. L. Beauchamp, *U.S. Patent 3,653,967.*
32 S. Le Bihan and M. Figlarz, *Electrochim. Acta, 18* (1973) 123.
33 S. Le Bihan, *Thèse,* Paris, 1974, No. CNRS AO 9424.
34 (a) M. Figlarz and S. Le Bihan, *C.R. Acad. Sci., Ser. C, 272* (1971) 50.
(b) S. Le Bihan and M. Figlarz, *Thermochim. Acta, 6* (1973) 319.
35 S. Le Bihan and M. Figlarz, *J. Cryst. Growth, 13/14* (1972) 458.
36 O. Glemser and J. Einerhand, *Z. Anorg. Allg. Chem., 261* (1950) 26.
37 C. Delmas, C. Fouassier and P. Hagenmuller, *Physica, 99 B* (1980) 81.
38 F. P. Kober, *J. Electrochem. Soc., 112* (1965) 1064.
39 F. P. Kober, *J. Electrochem. Soc., 114* (1967) 215.
40 H. Bode, K. Dehmelt and J. Witte, *Z. Anorg. Allg. Chem., 366* (1969) 1.
41 H. Bartl, H. Bode, G. Sterr and J. Witte, *Electrochim. Acta, 16* (1971) 615.
42 P. N. Bityutskii and V. I. Khitrova, *Sov. Phys.–Crystallogr., 13* (1968) 40, 867; *14* (1969) 99.
43 C. Delmas, C. Fouassier and P. Hagenmuller, *Mater. Res. Bull., 11* (1976) 1483.
44 G. W. D. Briggs, E. Jones and W. F. K. Wynne-Jones, *Trans. Faraday Soc., 51* (394) (1955) 1433; *52* (405) (1956) 1260.
45 C. Delmas, M. Devalette, C. Fouassier and P. Hagenmuller, *Mater. Res. Bull., 10* (1975) 393.
46 R. Barnard, C. F. Randell and F. L. Tye, *J. Electroanal. Chem., 119* (1981) 17.
47 D. Tuomi, *J. Electrochem. Soc., 112* (1965) 1.
48 S. E. S. El Wakkard and E. S. Emara, *J. Chem. Soc., 4* (1953) 3504.
49 R. Barnard, G. T. Crickmore, J. A. Lee and F. L. Tye, *J. Appl. Electrochem., 10* (1980) 61.
50 N. Yu. Uflyand, A. M. Novakovski, Yu. M. Pozin and S. A. Rozentsveig, *Elektrokhimiya, 2* (1966) 234; *3* (1967) 537.
51 J. J. Braconnier, C. Delmas, C. Fouassier and P. Hagenmuller, *Mater. Res. Bull., 15* (1980) 1797.
52 K. Mizushima, P. C. Jones, P. J. Wiseman and J. B. Goodenough, *Mater. Res. Bull., 15* (1980) 783.
53 C. Delmas, unpublished results.
54 B. E. Conway and P. L. Bourgault, *Can. J. Chem., 37* (1959) 292; *38* (1960) 1557; *40* (1962) 1690. *Trans. Faraday Soc., 58* (1962) 593.
B. E. Conway and E. Gileadi, *Can. J. Chem., 40* (1962) 1933.
55 R. Barnard, C. F. Randell and F. L. Tye, *J. Appl. Electrochem., 10* (1980) 109, 127.
56 R. W. Bramham, R. J. Doran, S. E. A. Pomroy and J. Thomson, in D. H. Collins (ed.), *Power Sources 1977,* Academic Press, London, p. 129.
57 E. Prikryl, O. Rademacher and K. Wiesener, *Z. Phys. Chem., 258* (1977) 113.
58 M. Paskiewicz and I. Walas, *Electrochim. Acta, 24* (1979) 629.
59 B. E. Conway, M. A. Sattar and D. Gilroy, *Electrochim. Acta, 14* (1969) 677, 695, 711. *J. Electroanal. Chem., 19* (1968) 351.
60 P. W. T. Lu and S. Srinivasan, *J. Electrochem. Soc., 125* (1978) 1416.
C. R. Davidson and S. Srinivasan, *J. Electrochem. Soc., 127* (1980) 1060.
M. H. Miles, G. Kissel, P. W. T. Lu and S. Srinivasan, *J. Electrochem. Soc., 123* (1976) 332.
61 G. Bronoel and J. Reby, *Electrochim. Acta, 25* (1980) 973.
62 E. A. Khotskaya, A. S. Kolosov and V. V. Polishchuk, *Elektrokhimiya, 7* (1971) 1064.
63 D. M. McArthur, in D. H. Collins (ed.), *Power Sources, 3,* Oriel Press, Newcastle upon Tyne, 1971, p. 91.
D. M. McArthur, *J. Electrochem. Soc., 117* (1970) 422, 729.
64 H. Gomez Meier, J. R. Vilche and A. J. Arvia, *J. Appl. Electrochem., 10* (1980) 611.
65 A. de Guibert, unpublished results.
66 V. P. Tysyachnyi, O. S. Ksenzhek and L. M. Pototskaya, *Elektrokhimiya, 8* (1972) 1692.

67 G. W. D. Briggs and M. Fleischmann, *Trans. Faraday Soc., 62* (1966) 3217; *67* (1971) 2397.
68 Z. Takehara, M. Kato and S. Yoshizawa, *Electrochim. Acta, 16* (1971) 833.
69 G. Feuillade and R. Jacoud, *Electrochim. Acta, 14* (1969) 1297.
70 J. Labat, *Thèse,* Bordeaux, 1965.
71 S. A. Aleshkevich, E. I. Golovchenko, V. P. Morozov and L. N. Sagoyan, *Elektrokhimiya, 4* (1968) 1237.
72 I. A. Dibrov and T. V. Grigor'eva, *Elektrokhimiya, 13* (1977) 979; *15* (1979) 281.
73 V. M. Vogel, *Electrochim. Acta, 13* (1968) 1815.
74 O. G. Malandin, I. S. Shamina, S. M. Rakhovskaya, I. K. Kuchkaeva, L. N. Sal'kova, A. V. Vasev, P. N. Bityutskii, G. V. Suchkova and L. A. Vereshchagina, *Elektrokhimiya, 10* (1974) 1571, 1745; *12* (1976) 573; *14* (1978) 1380; *16* (1980) 1041.
75 M. A. Aia, *J. Electrochem. Soc., 114* (1967) 418.
76 E. J. Rubin and R. Baboian, *J. Electrochem. Soc., 118* (1971) 428.
77 P. Kelson, A. D. Sperrin and F. L. Tye, in D. H. Collins (ed.), *Power Sources 4,* Academic Press, London, 1973.
78 R. Bonnaterre-Saft, unpublished results.
79 J. P. Harivel, B. Morignat, J. Labat and J. F. Laurent, in D. H. Collins (ed.), *Power Sources 1966,* Academic Press, London, p. 239.
80 R. Barnard, C. F. Randell and F. L. Tye, *J. Appl. Electrochem., 11* (1981) 517.
81 Yu. M. Guliamov, M. D. Dolgushin and L. N. Sagoyan, *Elektrokhimiya, 7* (1971) 896.
82 N. Yu. Uflyand, S. V. Mendeleva and S. A. Rozentsveig, *Elektrokhimiya, 6* (1970) 1312.
83 E. A. Kaminskaya, N. Yu. Uflyand and S. A. Rozentsveig, *Elektrokhimiya, 7* (1971) 1839.
84 L. D. Dyer, B. S. Borie and G. P. Smith, *J. Am. Chem. Soc., 76* (1954) 1499.
85 D. Tuomi and G. J. B. Crawford, *J. Electrochem. Soc., 115* (1968) 450.
86 J. P. Harivel, *Thèse,* Strasbourg, 1969.
87 E. J. Casey, A. R. Dubois, P. E. Lake and W. J. Moroz, *J. Electrochem. Soc., 112* (1965) 371.
88 R. J. Doran, in D. H. Collins (ed.), *Batteries: Proc. 3rd Int. Symp.,* Pergamon Press, London, 1963, p. 105.
89 D. F. Pickett and J. T. Maloy, *J. Electrochem. Soc., 125* (1978) 1026.
90 P. Ness, *Conferences SIE, Keilkeim, 1973.*
91 J. P. Cittanova, personal communication.